Observation of a cascaded process in intracavity terahertz optical parametric oscillators based on lithium niobate

C. L. Thomson* **and M. H. Dunn**
J. F. Allen Research Laboratories, School of Physics & Astronomy, University of St Andrews, North Haugh, St Andrews, Fife, KY16 9SS, UK
*cl t6@st-andrews.ac.uk

Abstract: Cascaded difference frequency generation has been observed in intracavity optical parametric oscillators based on bulk lithium niobate and producing nanosecond pulses of terahertz radiation. Two idler waves are generated, namely: the primary idler wave associated with the parametric down conversion process itself; and a secondary idler wave, due to difference frequency generation. Experimental investigations of the frequency, temporal evolution, propagation direction, intensity, phase matching and oscillation threshold of the generated down-converted waves are reported. The overall generation efficiency for the terahertz radiation is enhanced, thereby overcoming the Manley-Rowe limit. Advantages of the present approach over schemes based on periodically poled lithium niobate are identified.

OCIS codes: (190.0190) Nonlinear optics; (190.4970) Parametric oscillators and amplifiers; (190.4360) Nonlinear optics and devices; (190.2620) Frequency conversion; (140.3480) Lasers, diode-pumped; (999.9999) Terahertz generation.

References and links

1. J. M. Yarborough, S. S. Sussman, H. E. Puthoff, R. H. Pantell, and B. C. Johnson, "Efficient, tunable optical emission from $LiNbO_3$ without a resonator," Appl. Phys. Lett. **15,** 102–105 (1969).
2. M. A. Piestrup, R. N. Fleming, and R. H. Pantell, "Continuously tunable submillimeter wave source," Appl. Phys. Lett. **26,** 418–421 (1974).
3. K. Imai and K. Kawase, "A frequency-agile terahertz-wave parametric oscillator," Opt. Express **8,** 699–704 (2001).
4. G. Kh. Kitaeva, "Terahertz generation by means of optical lasers," Laser Phys. Lett. **5,** 559-576 (2008).
5. T. Edwards, D. Walsh, M. Spurr, C. Rae, and M. Dunn, "Compact source of continuously and widely-tunable terahertz radiation," Opt. Express **14,** 1582–1589 (2006).
6. D. J. M. Stothard, T. J. Edwards, D. Walsh, C. L. Thomson, C. F. Rae, M. H. Dunn, and P. G. Browne, "Line-narrowed, compact and coherent source of widely tunable terahertz radiation," Appl. Phys. Lett. **92,** 141105-1–141105-3 (2008).
7. D. Walsh, D. J. M. Stothard, T. J. Edwards, P. G. Browne, C. F. Rae, and M. H. Dunn, "Injection-seeded intracavity terahertz optical parametric oscillator," J. Opt. Soc. Am. B **26,** 1196–1202 (2009).
8. D. A.Walsh, P. G. Browne, M. H. Dunn, and C. F. Rae,"Intracavity parametric generation of nanosecond terahertz radiation using quasi-phase-matching," Opt. Express **18,** 13951–13963 (2010).
9. D. Molter, M. Theuer and R. Beigang, "Nanosecond terahertz optical parametric oscillator with a novel quasi phase matching scheme in lithium niobate," Opt. Express **17,** 6623–6628 (2009).
10. R. Sowade, I. Breunig, I. Camara Mayorga, J. Kiessling, C. Tulea, V. Dierolf, and K. Buse, "Continuous-wave optical parametric terahertz source," Opt. Express **17,** 22303–22310 (2009).
11. I. Breunig, R. Sowade, J. Kiessling, and K. Buse, "Higher-order cascaded processes in continuous-wave optical parametric oscillators," in *CLEO/Europe and EQEC 2011 Conference Digest,* OSA Technical Digest (CD) (Optical Society of America, 2011), paper CD11-5.

#191817 - $15.00 USD Received 10 Jun 2013; revised 6 Jul 2013; accepted 8 Jul 2013; published 16 Jul 2013

12. J. E. Schaar, K. L. Vodopyanov, and M. M. Fejer, "Intracavity terahertz-wave generation in synchronously-pumped optical parametric oscillators using quasi-phase-matched GaAs," Opt. Lett. **32,** 1284–1286 (2007).
13. K. L. Vodopyanov, "Optical THz-wave generation with periodically-inverted GaAs," Laser & Photonics Reviews **2,** 11–25 (2008).
14. K. Kawase, J. Shikata, H. Minamide, K. Imai, and H. Ito, "Arrayed silicon prism coupler for a terahertz-wave parametric oscillator," Appl. Opt. **40,** 1423–1526 (2001).
15. D. E. Zelmon, D. L. Small, and D. Jundt, "Infrared corrected Sellmeier coefficients for congruently grown lithium niobate and 5 mol.% magnesium oxide –doped lithium niobate," J. Opt. Soc. Am. B **14,** 3319–3322 (1997).
16. L. Pálfalvi, J. Hebling, J. Kuhl, A. Péter, and K. Polgár, "Temperature dependence of the absorption and refraction of Mg-doped congruent and stoichiometric $LiNbO_3$ in the THz range," Appl. Phys. Lett. **97,** 123505 (2005).

1. Introduction

Considerable progress has been made in recent years in opening up the terahertz (THz) spectral range (0.3 – 10THz) of the electromagnetic spectrum; a range that lies between the microwave and the infrared regions, and where there are many important potential applications in science, technology, engineering and medicine. Significant innovations have been made with regard to both sources and detectors, including in the present context the use of optical parametric generation techniques, based on the early pioneering work of Pantell and Puthoff [1, 2] and further extended more recently by Kawase [3] - see the extensive review paper by Kitaeva [4].

We previously reported a parametric device based on a novel intersecting cavity geometry [5] in which the nonlinear medium ($MgO:LiNbO_3$) used for the parametric generation of the terahertz radiation is located within the cavity of the pump laser, where it is subject to the high circulating intra-cavity field. Since this field is typically over an order of magnitude greater in intensity than the external field obtainable from the pump laser under optimum output coupling conditions, a device with a low oscillation threshold and significantly improved down-conversion efficiency results, while obviating the need for high-energy pump lasers. An additional advantage is that coupling optics between the pump laser and the parametric oscillator are eliminated, further contributing to the compactness of the device. Importantly the intersecting cavity geometry incorporates a separate idler wave cavity, the optical axis of which may be independently rotated relative to the optical axis of the pump wave cavity, hence retaining the advantages of the wide spectral coverage associated with angle tuning (0.5–4THz) as well a the rapid walk-off of the terahertz-wave, vital in view of the high absorption losses for this wave shown by the nonlinear medium. Typically 20nJ of extracted THz energy is obtained in a single pulse of duration around 10ns, implying a peak extracted THz power of the order of 2W, which at a pulse repetition rate of 0.5kHz corresponds to a mean extracted THz output power of the order of 10μW. On the basis of typical observed pump-pulse depletion due to parametric down conversion of the order of 50% and for pump-pulse energies of the order of 1mJ, conditions appropriate to the above stated performance figures, the generated THz energy per pulse is of the order of 3μJ. The large discrepancy between generated and extracted THz energy/power is a consequence of the aforementioned exceedingly high absorption losses encountered by THz radiation in the nonlinear medium; a problem that is generic to this class of device [4]. With simple optical components (off-axis parabolic reflector/cylindrical Teflon lens) the extracted THz radiation can be formed into a circularly symmetric beam of reasonable spatial quality (M^2 values in the range 1.5 to 2). Further, we have reported spectral linewidth reduction from typical linewidths of 50 GHz for the basic device to $<$ 1GHz by using intracavity etalons [6], and to $\approx$ 100MHz by injection seeding techniques [7], while still retaining the full tuning range.

In the present communication we report the observation and study of a cascaded idler-wave effect in which, in addition to the primary idler-wave that accompanies the parametric generation of the terahertz-wave as the required signal-wave, a secondary idler-wave is also gen-

#191817 - $15.00 USD Received 10 Jun 2013; revised 6 Jul 2013; accepted 8 Jul 2013; published 16 Jul 2013

erated in the nonlinear crystal. Such cascading effects have been reported recently by both ourselves and others, but only in those cases where periodically-poled nonlinear materials have been used in order to maintain collinear propagation of the pump and idler waves involved. Particular cases include: (i) in periodically-poled MgO:$LiNbO_3$ (PPLN) using an intra-cavity geometry, generating nanosecond pulses [8]; (ii) in PPLN using a pump-enhanced geometry, generating nanosecond pulses [9]; (iii) in PPLN using a trapped signal-wave resonator, leading to continuous-wave generation [10, 11]; (iv) in quasi-phase-matched GaAs using intra-cavity difference frequency generation, generating picosecond pulses [12, 13]. However to our knowledge this is the first report of similar effects in bulk (un-poled) MgO:$LiNbO_3$ used in the original non-collinear phase-matching geometry. We report a comprehensive study of the effect, in particular identifying the nonlinear process leading to the secondary idler-wave as being one of difference frequency generation (DFG), for reasons to be discussed. Importantly DFG also results in the amplification of the terahertz-wave generated as the signal-wave in the primary process of parametric generation, thereby defeating the Manley-Rowe limit, as widely recognised. We will contrast the different phase-matching geometries associated with the use of poled and un-poled nonlinear materials, and explore opportunities for increasing the terahertz radiation generation efficiency through further enhancement of the DFG process.

2. Experimental device

The device under consideration is shown in Fig. 1. The pump laser gain medium (LG) is a Nd:YAG crystal, 7mm in length and 4mm wide with a doping level of Nd at 1.3%. A fibre-coupled AlGaAs pulsed laser diode delivering pulses of 250μs duration and having peak powers up to 100W at a repetition rate of 135 Hz and at a wavelength of 803.7 nm is used to optically excite the gain medium. A standard electro-optic configuration based on a Pockels cell, quarter-wave plate and linear polariser is incorporated into the cavity for the purpose of Q-switching (QS). Mirrors M1 and M2 form the cavity for the pump-wave, with M1 and M2 having reflectivities of $> 99\%$ and 98% respectively. Mirrors M3, M4 and M5 form the cavity for the primary idler-wave, with M3, M4 and M5 having a reflectivity of $> 99.9\%$, $> 99.9\%$ and 60% respectively. The nonlinear medium (LN) is a MgO-doped $LiNbO_3$ crystal of length 70mm and cross-section 5mm$\times$5mm, with a doping level of 5*mol*%. The wavelength of the primary idler-wave, and hence the wavelength of the terahertz-wave, can be tuned in the usual way by changing the angle between the optical axis of the pump-wave cavity and the optical axis of the idler-wave cavity, this being effected by altering the angles of mirrors M3 and M5, thereby altering the propagation direction of the primary idler-wave within the crystal and hence altering the phase-matching condition. The generated terahertz radiation is extracted from the nonlinear crystal using an array of silicon prisms (SPA) as previously described by Kawase et

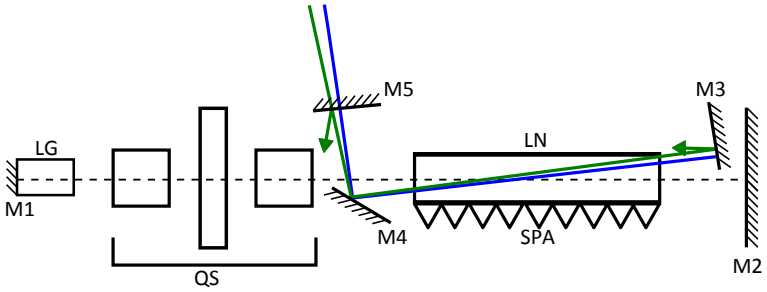

Fig. 1. Schematic diagram of the intracavity terahertz OPO.

#191817 - $15.00 USD Received 10 Jun 2013; revised 6 Jul 2013; accepted 8 Jul 2013; published 16 Jul 2013

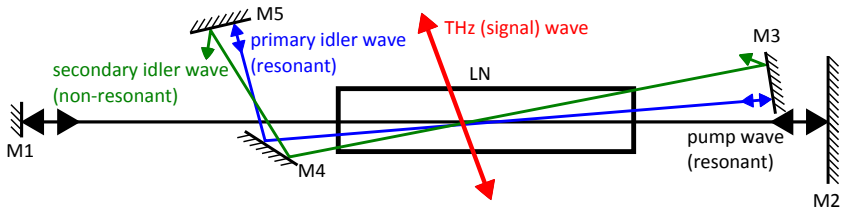

Fig. 2. Simplified schematic showing the propagation directions of the pump, idler and terahertz waves.

al [14]. Typically the spectral width of the primary idler-wave, and hence the accompanying THz radiation, is $\approx$ 50GHz (FWHM). A fuller description of this device and its performance characteristics is given in [5].

In the current investigation we have observed for the first time that a secondary idler-wave is generated in the above configuration. Figure 2 is an idealised diagram showing the cavity geometry in the vicinity of the nonlinear crystal in greater detail but also with the relevant angles greatly magnified compared with the actual situation in practice in order to more clearly illustrate the principles involved. In particular it may be seen that this secondary idler-wave propagates at an angle to the primary idler-wave (and also the pump-wave), such that the two idler-waves become spatially separated after propagating several centimetres beyond mirror M5, allowing their individual spectral and temporal characteristics, in addition to the angle between them, to be measured. Due to this angular separation only the primary idler-wave (namely that idler-wave produced by the primary parametric process itself) is resonated in the idler-wave cavity since the secondary idler-wave is not incident on the mirrors, M3 and M5 at 90°. The power in the secondary idler-wave is therefore generated on only a single pass of the nonlinear crystal. (It should be noted that as expected two secondary idler-waves are independently generated, these propagating in opposing directions.)

3. Observation of the secondary idler-wave

The propagation direction of the primary idler-wave is determined by the optical axis of the idler-wave cavity, which is a standing-wave cavity formed by mirrors M5-M4-M3. The propagation direction of the secondary idler-wave is undefined by any external constraints, as mentioned previously, and is therefore determined by the phase matching condition alone. (There is of course a counter-propagating secondary idler-wave in addition to the one shown, as discussed above.) Mirror M4 is such that a small fraction of the pump-wave intensity is reflected out of the pump-wave cavity for the purposes of monitoring. By using a single optical fibre positioned beyond M5, feeding into an optical spectrum analyser (OSA, model HP86140A) it was possible both to determine the spectral content of each of the three waves separately as well as to determine the angle between the primary and secondary idler-waves as generated within the nonlinear crystal (provided that the refraction occurs at the crystal end faces is taken into account). In addition, by using a large-aperture collection optic all three beams could be simultaneously imaged onto the optical fibre input to the OSA, so allowing the OSA to monitor all three beams simultaneously and hence to directly measure their wavelength/frequency differences. The (vacuum) wavelengths as measured by the OSA were converted into frequencies for the convenience of subsequent analysis. The resolution bandwidth of the OSA was $\approx$ 50GHz (FWHM), comparable to the actual linewidth of the primary idler-wave.

#191817 - $15.00 USD Received 10 Jun 2013; revised 6 Jul 2013; accepted 8 Jul 2013; published 16 Jul 2013

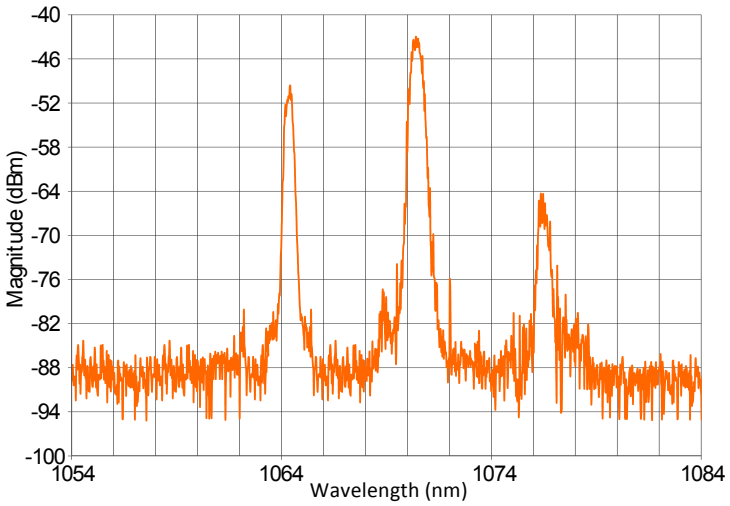

Fig. 3. Typical OSA trace showing the pump, primary idler and secondary idler waves.

4. Investigation of idler-waves

4.1. Frequencies of idler-waves

The frequency of the pump-wave is 281.68THz (corresponding to the vacuum wavelength of 1064.3nm) and is constant throughout. The frequency of the primary idler-wave was tuned from around 280.7THz (1068nm) to around 279.7THz (1072nm) by altering the angles of mirrors M3 and M5. This corresponds to tuning the frequency of the terahertz radiation generated by the parametric process over the range 1 to 2THz. Using the OSA as described previously, the frequencies of both the primary and secondary idler-waves were measured at a number of points across the tuning range. A typical OSA trace is displayed in Fig. 3 and the deduced results are presented in table 1. The frequency difference between the pump-wave and the primary idler-wave immediately gives the frequency of the terahertz radiation generated by the parametric process, as tabulated in column 3 of table 1. The measured frequency difference between the primary and secondary idler-waves is also displayed in column 4 of table 1. In Fig. 4 this second frequency difference is plotted against the first frequency difference (itself the frequency of the terahertz radiation), accompanied by the curve (straight line) corresponding to equality of these two frequency differences. The near equality shown (to within measurement capability) by these frequency differences at each point in the tuning range is consistent with the secondary idler-wave being generated by the process of difference frequency generation (DFG) in which the terahertz-wave, which is parametrically generated as a result of the interaction of the primary idler-wave with the pump-wave, then subsequently interacts with the primary idler-wave so as to generate the secondary idler-wave, at the difference frequency, hence accompanied by the amplification of the terahertz radiation that was initially generated parametrically in the primary process. Averages of the residuals calculated from Fig. 4 are (0.0 ± 0.06), consistent with the accuracy of measurement and linewidths, as previously discussed.

4.2. Phase matching for difference frequency generation

We now consider the phase matching schemes involved in these processes, as depicted in Fig. 5, in order to assess the viability of the process of difference frequency generation.

The relationship between the pump, idler and terahertz frequencies in the original parametric

#191817 - $15.00 USD Received 10 Jun 2013; revised 6 Jul 2013; accepted 8 Jul 2013; published 16 Jul 2013

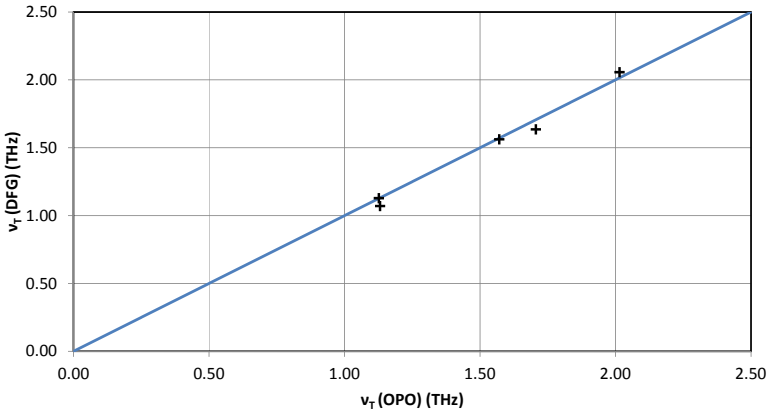

Fig. 4. Graph comparing the frequency differences for the DFG process with those for the parametric process, along with a straight line indicating equality.

process is:

$$\nu_p = \nu_{i1} + \nu_T \tag{1}$$

where the subscripts *p, i1* and *T* denote the pump-wave, primary idler-wave and terahertz-wave respectively. The magnitudes of the corresponding wave vectors (within the nonlinear medium) are calculated using the following equation:

$$k_j = \frac{2\pi n_j \nu_j}{c} \tag{2}$$

where the subscript j indicates the wave of interest, and n_j is the refractive index for that wave.

In Fig. 5 the triangle ADC describes the phase matching for the primary process of optical parametric oscillation which leads to the generation of the terahertz-wave along with the primary idler-wave. The angle DAC is defined internally as being the angle, within the nonlinear medium, between the optical axes of the cavities associated with pump-wave and primary idler-wave, as described previously. By measuring the vacuum wavelengths of the primary idler-wave and the pump-wave their associated frequencies can be determined, and then knowing the refractive indices associated with these frequencies [15], values for k_{i1} and k_p within the nonlinear

Table 1. Summary of results from OSA measurements of the primary and secondary idler-waves. The wavelength of the pump laser was fixed at 281.68THz.

ν_{i1} (THz)	ν_{i2} (THz)	OPO ν_T (THz)	DFG ν_T (THz)
280.55	279.48	1.13	1.07
280.56	279.43	1.12	1.13
280.11	278.55	1.57	1.56
279.97	278.34	1.71	1.63
279.67	277.61	2.02	2.05

#191817 - $15.00 USD Received 10 Jun 2013; revised 6 Jul 2013; accepted 8 Jul 2013; published 16 Jul 2013

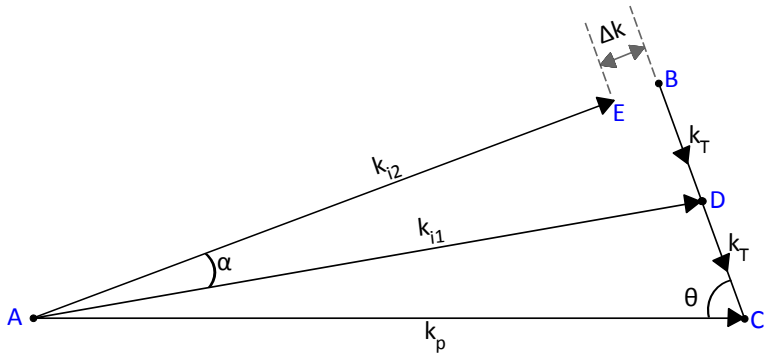

Fig. 5. Phase matching condition corresponding to parametric generation of the primary idler and terahertz waves along with DFG of the secondary idler by the mixing of the terahertz and primary idler waves.

medium may be readily calculated by using Eq. (2) above. Knowing the refractive index associated with the terahertz frequency [16] then allows k_T to be calculated in the same manner. The magnitudes of the three wave vectors so deduced and the angle DAC as externally defined should then be consistent with the closure of the phase matching triangle ADC, thereby corresponding to perfect phase matching as shown in Fig. 5.

In the secondary step the terahertz radiation generated in the primary process then undergoes DFG with the primary idler-wave also generated in the primary process, so as to generate further terahertz radiation at the same frequency and in the same direction as that generated in the primary process (i.e. to amplify the existing terahertz radiation). In the phase matching diagram this means that the length BD (representing the terahertz-wave vector as engaged in the secondary process) is put equal in magnitude to and collinear with the length DC, and located as shown. In addition, radiation is generated at a new frequency, i.e. the difference frequency, namely:

$$\nu_{i2} = \nu_{i1} - \nu_T \tag{3}$$

This wave is, of course, the secondary idler-wave. Knowing the frequency of the secondary idler-wave, by using Eq. (3) above, and also its associated refractive index in the nonlinear medium, the magnitude of its wave vector, k_{i2}, can be calculated. This wave vector although determined in magnitude is not constrained geometrically with regard to propagation direction, since there is no associated cavity, and hence it may assume a direction such as to minimise the phase mismatching associated with the secondary process. This corresponds to taking up the direction along the line AB as shown in Fig. 5, when the phase mismatching associated with the secondary process, Δk, is then given by the length EB. In summary, both the magnitudes and the directions of the wave vectors k_{i1} and k_T, along with the magnitude alone of the wave vector of k_{i2}, are fixed by the primary process of parametric generation, while the direction of k_{i2} is determined through optimisation of the phase matching for the secondary process of DFG.

Figure 5 enables the magnitude of the phase mismatching involved in the secondary process to be evaluated. Applying the cosine rule to the triangle ABC in relation to the angle θ we obtain:

$$(AB)^2 = k_p^2 + (2k_T)^2 - 4k_p k_T \cos\theta \tag{4}$$

And applying the cosine rule to the triangle ADC in relation to the angle θ we obtain:

$$k_{i1}^2 = k_p^2 + k_T^2 - 2k_p k_T \cos\theta \tag{5}$$

#191817 - $15.00 USD Received 10 Jun 2013; revised 6 Jul 2013; accepted 8 Jul 2013; published 16 Jul 2013

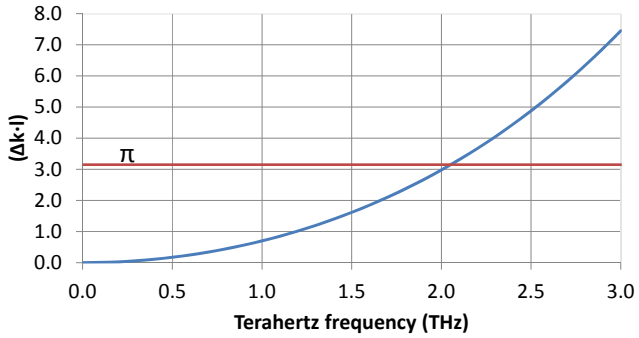

Fig. 6. Graph of $(\Delta k \cdot l)$ as a function of the terahertz frequency, for l=1mm. The line $\Delta k \cdot l = \pi$ is also indicated.

Using Eq. (5) to eliminate the $\cos\theta$ term present in Eq. (4) results in an expression for AB that depends only on the wave vectors, namely:

$$AB = \sqrt{\left(2k_T^2 - k_p^2 + 2k_{i1}^2\right)} \tag{6}$$

Hence we can now determine the length EB, which corresponds to the phase mismatching Δk as:

$$\Delta k = EB = \sqrt{\left(2k_T^2 - k_p^2 + 2k_{i1}^2\right)} - k_{i2} \tag{7}$$

The question remains as to whether the terahertz radiation generated through the secondary process of DFG starts off in phase with the terahertz radiation generated through the primary process of parametric generation thereby resulting in the terahertz field generated in the primary process being amplified from the start by the secondary process, this being consistent with DFG. That this is indeed the case can be readily shown by using the standard coupled rate equations of second order nonlinear optics to determine the relative phases of the fields at the start of their generation. Obviously phase mismatching then subsequently results from the propagation of the waves through the nonlinear medium, this being determined by the value of Δk as calculated using Eq. (7). A useful criterion for the impact of phase mismatching on generation efficiency not being too severe is to require that:

$$\Delta k \cdot l \leq \pi \tag{8}$$

where l is the distance over which the waves interact. We now explore the magnitude of the phase mismatching encountered in the present device. Because of the rapid walk-off of the terahertz-wave from the pump-wave and idler-waves the interaction length is of the order of the beam diameters, in this present case this being approximately 1mm. In order to calculate Δk using Eq. (7), we require knowledge of the refractive indices experienced by the waves involved within the nonlinear medium. For the case of the pump-wave and the two idler-waves we have used the values given in [15]; note that the refractive index may be taken as the same for all three of these waves in view of the closeness of their frequencies (i.e. $n_p = n_{i1} = n_{i2} = n_0$). For the case of the terahertz-wave we have used the values given in [16].

The procedure is then as follows: (i) knowing the vacuum wavelength of the pump-wave (1064.3nm in the present case) calculate the frequency of the pump-wave, ν_p; (ii) knowing the refractive index associated with the pump-wave in the nonlinear gain medium, n_0, calculate the magnitude of the wave vector of the pump-wave in the gain medium, k_p; (iii) choose a particular

#191817 - $15.00 USD Received 10 Jun 2013; revised 6 Jul 2013; accepted 8 Jul 2013; published 16 Jul 2013

Table 2. Comparison of calculated and measured values of angle α (see Fig. 5).

Terahertz frequency (THz)	α (calculated)	α (measured)
1.8	1.48	1.42
2.2	2.01	2.10

terahertz frequency, ν_T , and calculate the magnitude of its associated wave vector, k_T, knowing the associated refractive index, n_T; (iv) now calculate the frequencies of the accompanying primary and secondary idler-waves, ν_{i1}, ν_{i2}; (v) knowing the refractive index, n_0, associated with these idler-waves calculate the magnitudes of their wave vectors, k_{i1}, k_{i2}; (vi) now use the determined magnitudes of the wave vectors to calculate the magnitude of the phase mismatch using Eq. (7).

Figure 6 displays the resulting plot of $\Delta k \cdot l$ (with $l = 1mm$) as a function of terahertz frequency. It may be seen that throughout the frequency range of interest here (1–2THz) the value of $\Delta k \cdot l$ remains below the critical value of π and this gives further credence to the secondary process being one of DFG. However, on increasing the terahertz frequency further $(\Delta k \cdot l)$ is predicted to continue to increase, reaching 2π at around 2.8THz. It should be noted that the phase mismatching arises from the difference in the refractive index experienced by the terahertz wave compared with that experienced by the pump and idler waves. It may readily be shown that if all refractive indices are the same then Δk is zero, independently of the frequency of the terahertz wave. An approximate, but valid, expression for calculating Δk directly is:

$$\Delta k = \frac{2\pi n_0}{c} \cdot \left[\left(\frac{n_T}{n_0} \right)^2 - 1 \right] \cdot \frac{\nu_T^2}{\nu_p} \tag{9}$$

4.3. Propagation directions of the idler waves

The analysis discussed in the previous section concerning phase matching conditions can be readily extended to predict the propagation of the secondary idler-wave relative to the primary idler-wave, namely:

$$\cos\alpha = \frac{AB^2 + k_{i1}^2 - k_T^2}{2 \times AB \times k_{i1}} \tag{10}$$

where α is the angle between the propagation directions of the two idler waves within the nonlinear medium. Since this angle is very small ($\approx 1^\circ$, see Fig. 5), Eq. (10) may be approximated to the convenient expression:

$$\alpha = \sqrt{\frac{k_T^2 - (AB - k_{i1})^2}{AB \times k_{i1}}} \tag{11}$$

where α is now expressed in radians. In general the first term in the numerator dominates over the second term, and hence this second term may usually be neglected. Shown in table 2 are the values of α calculated under the conditions stated, using Eq. (11), as well as two experimentally measured values.

The agreement of the experimentally measured values with the calculated values is reasonable considering the difficulties inherent in measuring such small angles. Overall the general trends shown further confirm DFG as being the underlying process resulting in the generation of the secondary idler-wave, with the accompanying amplification of the terahertz-wave.

#191817 - $15.00 USD Received 10 Jun 2013; revised 6 Jul 2013; accepted 8 Jul 2013; published 16 Jul 2013

4.4. *Temporal evolution of the pump-wave and idler-waves*

Figure 7 shows the temporal evolution of the pump pulse and the two idler pulses. Figure 7(a) compares the time development of the primary idler pulse with that of the pump pulse, from which it can be seen that the onset of the primary idler pulse is delayed some 10ns after the onset of the pump pulse from which it is derived. This is of course characteristic of the parametric oscillation process involved here in which initially only the pump-wave is present in the nonlinear medium, and the down-converted waves grow from noise through the optical gain induced in the nonlinear medium by the pump-wave. Typically, optical gains of the order of 140dB are required before coherent down-converted waves (the primary idler-wave in this case) become detectable. Hence there is a required build-up time before the pulse becomes detectable from noise, in this case of the order of 10ns. The build-up time in the present case is comparable to the duration of the pump-pulse itself (≈20ns, FWHM) and accounts for the shorter duration of the generated idler pulse (≈10ns, FWHM).

Figure 7(b) compares the temporal development of the secondary idler pulse with that of the primary idler pulse. In this case the secondary idler pulse is seen to start simultaneously with the primary idler pulse, and to grow in step with it. This is consistent with the secondary generation process being one of cascaded DFG. Under conditions appertaining in the present setup two coherent waves, namely the terahertz-wave and the primary idler-wave, are present simultaneously in the nonlinear medium and hence, subject to satisfactory phase matching as previously discussed, immediately generate radiation at their difference frequency; namely as the secondary idler-wave. In this process the terahertz-wave, initially generated by parametric oscillation, is amplified. Throughout there is no requirement to build up a coherent field from noise, and hence no delays through requiring a build-up time.

4.5. *Thresholds and pulse energies of pump and idler waves*

The pulse energy characteristics of the device with and without parametric down-conversion are displayed in Fig. 8 as a function of the pulse energy delivered by the laser diode. In the absence of parametric down-conversion (achieved by physically blocking the off-axis idler cavity) the energy of the pump pulse is seen to increase monotonically from the threshold of the laser at a laser diode energy of 5.5mJ to reach a value of around 1.7mJ for a laser diode energy of around 11mJ; this being followed by saturation of the energy of the pump pulse (probably due to thermal effects). When parametric down-conversion is allowed to take place, by unblocking the off-axis idler cavity, the energy of the pump pulse is observed to be clamped at around 0.7mJ, due to the onset of down-conversion, as indicated by the simultaneous growth in the primary

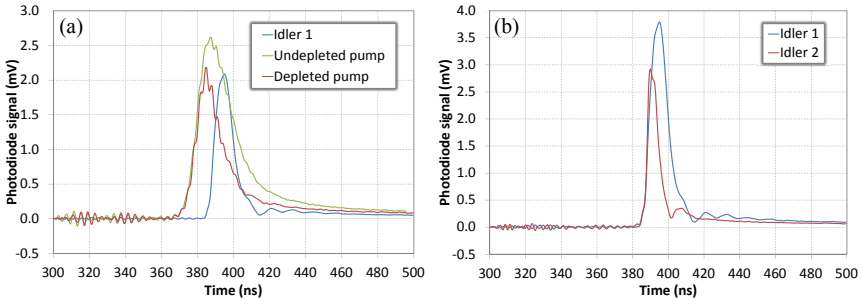

Fig. 7. Temporal profiles of the pump-wave, primary and secondary idler-waves. (a) The relative timing of the pump and primary idler waves. (b) The primary and secondary idler waves are generated simultaneously.

#191817 - $15.00 USD Received 10 Jun 2013; revised 6 Jul 2013; accepted 8 Jul 2013; published 16 Jul 2013

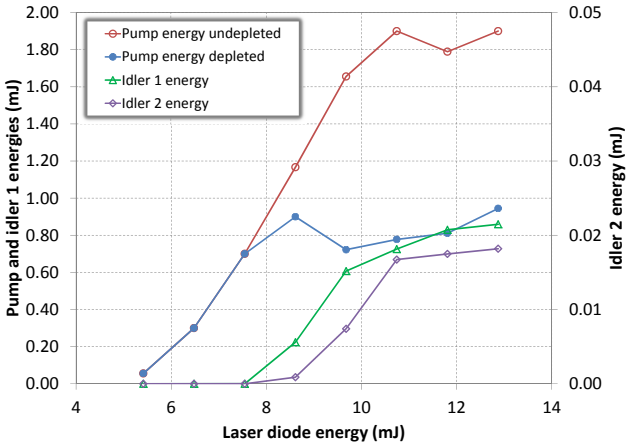

Fig. 8. Pump and idler energy measurements, showing the common threshold energy for the primary and secondary idler-waves.

idler pulse from a threshold at around 7.5mJ. Typically at pulse energies from the laser diode of around 10-11mJ, the pump pulse energy of around 1.7mJ is depleted by around 1mJ, hence corresponding to around 60% pump depletion, with around 0.8mJ of this energy appearing in the primary idler pulse. Such performance is highly satisfactory for this class of device. Also shown in Fig. 8 is the growth of the secondary idler pulse. The threshold for generation of the secondary idler pulse, of around 7.5mJ, is similar to that for the primary idler pulse. This is to be expected in that as previously discussed the process of cascaded DFG is not itself subject to a threshold unlike parametric generation, since both fields involved (the primary idler field and the terahertz field) are present in the nonlinear medium as a result of parametric generation and do not need further time to build up from noise.

Under the present circumstances the energy of the secondary idler pulse is substantially lower than that of the primary idler pulse, 0.02mJ (maximum) as opposed to 0.8mJ (maximum), indicating an accompanying enhancement of the generation efficiency for the terahertz radiation of only 2.5%. This is disappointingly small. We believe that a considerable improvement in efficiency could result from the provision of an additional cavity to enhance the generation of the secondary idler. In the present arrangement the secondary idler exits the nonlinear gain medium after only a single pass, there being no such cavity. This is to be contrasted with the situation in the case of terahertz generation based on quasi-phase matching, in which periodically-poled lithium niobate (PPLN) replaces the bulk lithium niobate used in the present arrangement, other features of the device remaining essentially the same; an approach reported by ourselves [8] as well as by Molter et al. [9]. In this approach the grating vector associated with the periodic poling allows all the fields involved, apart from the terahertz field which is still required to rapidly exit the nonlinear gain medium, to propagate in a collinear manner while still maintaining quasi-phase matching. As a consequence all fields can now be simultaneously resonated by a single cavity (essentially the pump-wave cavity). Enhancement efficiencies of the order of 10% have been reported in [8, 9] for such an arrangement. More recently we have been able to demonstrate efficiency enhancements of the order of 50% through further improvements in the nonlinear gain medium (PPLN). The additional cavity proposed to enhance the generation of the secondary idler in the case of bulk lithium niobate is anticipated to at least match the 50% enhancement seen in the case of PPLN and to lead to yet further improvements (see below).

The use of bulk lithium niobate in the non-collinear geometry has three important advan-

#191817 - $15.00 USD Received 10 Jun 2013; revised 6 Jul 2013; accepted 8 Jul 2013; published 16 Jul 2013

tages over the use of PPLN in the collinear geometry. Firstly the capability for angle tuning over a wide spectral range (0.5–4THz [5]) is retained; secondly the significant loss of the non-linear coefficient resulting from quasi-phase matching is avoided and finally the use of separate cavities as opposed to one common cavity provides the flexibility required for individual cavity optimisation. It is therefore important that cascaded processes for further overcoming the Manley-Rowe limit continue to be explored in the context of THz devices based on the use of bulk lithium niobate combined with non-collinear phase matching geometries. This, the first observation that the cascaded DFG process occurs under such circumstances even in the absence of a secondary idler cavity, is an encouraging start.

5. Conclusions

We have observed the presence of a secondary idler-wave in the optical parametric generation of terahertz radiation in bulk lithium niobate using a non-collinear phase matching scheme (often related to the generation of Cherenkov-radiation). No resonator is involved in the case of the secondary idler which is also non-collinear with the other waves present (pump-wave, primary idler-wave and terahertz-wave as the signal-wave). We have demonstrated that the source of the secondary idler-wave is a cascaded DFG process in which the primary idler-wave interacts with the terahertz signal-wave, both these waves being produced through optical parametric generation, so as to produce the secondary idler wave at the difference frequency, while simultaneously amplifying the terahertz signal-wave. We have demonstrated that in terms of the frequency spectrum, phase matching, angular separation of the idler-waves, temporal behaviour of the pump-wave and both idler-waves, and threshold behaviour, all are consistent with the DFG process. The cascaded process is significant in overcoming the efficiency constraints associated with the Manley-Rowe limit.

Acknowledgments

We would like to thank the Engineering and Physical Sciences Research Council (UK) for partial support of this work.

#191817 - $15.00 USD Received 10 Jun 2013; revised 6 Jul 2013; accepted 8 Jul 2013; published 16 Jul 2013